ELSEVIER

Thermochimica Acta 302 (1997) 77–85

thermochimica acta

Differential scanning calorimetry of the processing of VF_2/VF_3 copolymers

Isabelle George, Lawrence Judovits*

ELF Atochem North America, Inc., 900 First Avenue, P.O. Box 61536, King of Prussia PA 19406-0936, USA

Received 1 November 1996; received in revised form 4 April 1997; accepted 8 April 1997

Abstract

Poly(vinylidene fluoride-trifluoroethylene), VF_2/VF_3 random copolymers have been noted to exhibit ferroelectricity. To obtain a high level of piezoelectrical activity it is necessary for the copolymer to undergo additional processing. In this study differential scanning calorimetry (DSC) was used to follow the processing of this material for 81/19 and 76/24 mol% compositions. Although DSC peak parameters were found to show a relationship with piezoelectrical activity a leveling effect was noted. Additionally a cold crystallization effect was noted. This effect can be explained if one assumes the paraelectric phase to be a condis crystal transition. © 1997 Elsevier Science B.V.

Keywords: Condis crystal; DSC; Ferroelectricity; Piezoelectricity; Poly(vinylidene fluoride-trifluoroethylene)

1. Introduction

Poly(vinylidene fluoride-trifluoroethylene), VF_2/VF_3 random copolymers have been noted to exhibit ferroelectricity [1–3]. To achieve a high level of piezoelectrical activity it is necessary for the copolymer to undergo additional processing. Differential scanning calorimetry (DSC) was employed to follow the effects of the different elements of the processing.

To understand the processing of VF_2/VF_3 copolymers a brief discussion of the possible crystal forms is necessary. In order to do so a brief discussion of the homopolymers, polyvinylidene fluoride (PVDF) and polytrifluoroethylene (PtrFE), is first necessary.

1.1. PVDF crystal forms (just α and β)

At least five crystalline modifications of PVDF have been reported in the literature [4,5]. Of interest to this study are the α (form II) and β (form I) crystal structures. The α phase is the most common polymorph of PVDF since it is the one normally crystallized from the melt although other forms may be obtained depending on the nucleating agents present and crystallization conditions [6]. The α molecular conformation consists of repeating sequences of $TGT\overline{G}$ with a fiber identity period of 0.462 nm where T and G denote the trans and gauche skeletal torsional isomers, respectively. The unit cell has been found to be orthorhombic with lattice parameters of $a = 0.496$, $b = 0.964$, and $c = 0.462$ nm. Although the individual chains of the α phase possess a net electrical dipole, the chains pack so that their dipoles cancel resulting in a nonpolar unit cell. However, poling the α phase may result in obtaining the α_p phase [7,8]. The α_p phase has the same unit cell dimensions as the α phase except that its dipole vectors point in the same direction; thus its unit cell is polar and therefore exhibits piezoelectricity although the β phase has the higher activity [9].

*Corresponding author.

PII S0040-6031(97)00232-3

The β phase is the most piezoelectric form and is usually obtained by stretching the homopolymer at temperatures that appear to be below the α transition (as noted, e.g. in dynamic mechanical analysis, DMA) [10]. The chains take on essentially all-trans conformation with a repeating period of 0.256 nm [11]. The unit cell has been determined to be orthorhombic with lattice parameters $a = 0.858$, $b = 0.491$, and $c = 0.256$ nm. Since the chains pack in either a planar or near-planar zigzag, their dipoles all point (with the exception of defects) in the same direction; thus both the chain and the unit cell are polar. For a further discussion with detailed molecular and crystal structures, a review by Lovinger is suggested [4].

1.2. PtrFE crystal structure

Two separate molecular and crystal structures have been proposed for PtrFE. Lovinger and Cais [12] have suggested a crystal structure having a disordered conformation of TG, T$\overline{\text{G}}$ and TT groups with a fiber period of 0.229 nm and a hexagonal packing with $a = 0.561$ nm. Such a structure would be analogous to the high temperature paraelectric P(VF_2/VF_3) crystal structure (discussed in the next section). Equatorial d-spacings [12] are similar to those given by Higashihata et al. [13] and also probably to that of Gal'perin et al. [14], although Gal'perin et al. obtained a different fiber axis. A fiber axis similar to Lovinger and Cais [12] was, however, reported by Kolda and Lando [15]. Tashiro et al. [16] has suggested a crystal structure for PtrFE different than that of Lovinger and Cais [12]. They [16] proposed a disordered all-trans conformation with an orthorhombic unit cell having parameters $a = 0.968$, $b = 0.562$, and $c = 0.253$ nm. Such a structure may be similar to the cooled phase of P(VF_2/VF_3) copolymers (described in the next section).

A partial explanation of the conflicting results between Lovinger and Cais [12] and Tashiro et al. [16] may be found in a paper by Oka and Koizumi [17]. They found two different crystal phases being formed depending upon the supercooling used to crystallize PtrFE. If cooled slowly, a phase with a double x-ray diffraction (D phase) peak appeared; however, if quenched a single peak (S phase) was seen. The D phase was found to be orthorhombic with peaks at the (110) and (200) reflections while the S phase was found to be pseudohexagonal with a single unresolved (110, 200) peak.

Although one would think that the D and S phases would relate to crystal structures previously proposed [12,16], however, problems exist with such a correspondence. Calculated crystal density of Tashiro et al. [16] is lower than the bulk density of Oka and Koizumi [17] (crystal density determined by x-ray diffraction should be greater than the sample density). Thus the crystal model of Tashiro et al. [16] is not totally consistent with that of Oka and Koizumi [17]; however, neither is the model of Lovinger and Cais [12]. The crystal structure of Lovinger and Cais [12] is nonpolar while both phases of Oka and Koizumi [17] are polar. Additionally, Oka and Koizumi [17] suggested that their results corresponded better to the low temperature and cooled phase of VF_2/VF_3 copolymer studies of Tashiro et al. [16]. Lovinger and Cais [12], on the other hand, indicated that his PtrFE structure compared best to the copolymer's high temperature parelectric phase. (In support of the above contention by Lovinger and Cais [12], the d-spacings of Higashihata et al. [13] also indicate a similarity between the high temperature phase and the PtrFE crystal structure). Therefore it is difficult to recommend a crystal structure for PtrFE since it is still being debated in the literature and more work in this area will be necessary for the issue to be resolved.

1.3. VF_2/VF_3 copolymers

Three types of crystal phases have been identified for the copolymer [18,19]. Tashiro and Kobayashi [19] have denoted them as:

1. Low temperature (LT)
2. Cooled (CL)
3. High temperature (HT) phases.

The appearance of any of these phases is primarily dependent upon comonomer content, temperature and processing conditions. In general, the phase transitions seen may be summarized as follows [16]:

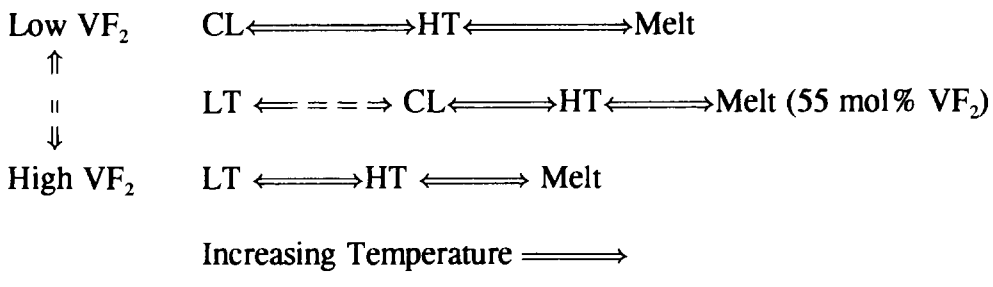

The dotted line in the above diagram indicates drawing or poling. The 55 mol% VF_2 copolymer illustrates all three phases and is schematically drawn in the middle in the above diagram.

1.4. Low temperature (LT) phase

The low temperature phase for the 55 mol% VF_2 copolymer has a crystal structure that is similar to the PVDF β form and therefore is piezoelectric [13]. Tashiro, et al. [16,20] suggest a monoclinic unit cell with dimensions $a = 0.912$, $b = 0.525$, and $c = 0.255$ nm, with $\beta = 93°$. In an orthorhombic system all angles in a unit cell equal 90°. The addition of VF_3 segments slightly distorts the unit cell resulting in an approximately 3° expansion in the β angle. (The β angle referred to is one of three angles found in a unit cell; this is not to be confused with PVDF β crystalline form or β transition.) Lovinger et al. [21,22] have also found the low temperature phase (at 52 mol % VF_2) to be analogous to β–PVDF; however, they deduced a hexagonal packing although their reported d-spacings are similar to Tashiro et al. [16,20]. Also, as would be expected, Lovinger's group found that as the VF_2 content increased, the unit cell became more compact. That is, for 65, 73 and 78 mol % VF_2 the axial length decreases from 0.524 to 0.516 to 0.512 nm, respectively [23,24]. Legrand [25] proposed a structure in between that of Tashiro's [16,20] and Lovinger's [21,22] groups. He found for a 70 mol % VF_2 copolymer a pseudohexagonal unit cell with parameters of approximately $a = 0.901$ and $c = 0.224$ nm at 20°C. The b axis was found to exhibit a temperature dependent $a/\sqrt{3}$ relationship. Thus, though the a axis did not equal the b axis, as required for a true hexagonal close packing, it is specified by the above relationship.

In general, all the above investigators found the LT phase similar to the β phase of PVDF except with a slightly expanded unit cell. As implied by being similar to the β phase, the chains pack in an all-trans conformation and the phase is piezoelectric. Since the LT phase can undergo a Curie transition to a high temperature paraelectric phase, it is also ferroelectric.

1.5. High-temperature (HT) phase

The HT phase for the VF_2/VF_3 copolymer is similar to that of the α phase although it is also paraelectric [26]. For the 55 mol% VF_2, Tashiro suggests an orthorhombic unit cell with parameters $a = 0.975$, $b = 0.563$, and c (fiber axis) $= 0.460$ nm [16,20]. Tashiro et al. also note an a/b ratio of $\sqrt{3}$ suggestive of a hexagonal symmetry. Lovinger, et al. hypothesize only an expanded LT pseudo-hexagonal lattice with molecular chains assuming irregular TG, $T\overline{G}$ and TT sequences similar to PVDF's α phase [21,22]. Legrand, in the middle, gives a pseudo-hexagonal lattice with approximate dimensions of $a = 0.980$ (at 100°C) and $c = 0.255$ nm with b equal to $a/\sqrt{3}$. Legrand's structure is very similar to the initial structure of Tashiro et al. [27] which was proposed in 1981 but altered in 1984 [16,20] (Tashiro, et al. also initially suggested that the LT phase was orthorhombic) [27]).

Although the α phase of PVDF is similar to the HT phase, they are different crystal forms and in no way should the α phase be considered the paraelectric counterpart to β-PVDF. The α phase is not polar, its unit cell is instead antipolar and therefore not paraelectric. Also, the α form will not transform spontaneously to the ferroelectric β phase at lower temperatures. As a matter of fact, Lovinger et al. [28] have shown that at high defect levels annealing at high temperature results in the crystallization of the β phase from the α phase. Although PVDF containing 13.5 to 15.5 mol% regiodefects exhibits a Curie transition

from the ferroelectric β to the paraelectric HT phase, at a lower inversion level of 11.4 mol% a solid-state transition (on heating) from the antipolar α phase to the paraelectric HT phase was noted. Thus the 11.4 mol% defect PVDF exhibits both the α and HT phases. Therefore, although a similarity exists between the HT and α phases, they are two distinct phases.

1.6. Cooled (CL) phase

The poled phase is thought by Lovinger et al. [21,22] to be a mixture of the LT and HT phases with some structural irregularity. Horiuchi et al. [29] also give a similar interpretation. However, Tashiro et al. [16,20] have a different interpretation. That is, the CL phase forms a disordered superstructure having a subcell structure similar to the LT phase. The monoclinic unit cell constants for the subcell structure are $a = 0.916$, $b = 0.543$, and c (fiber axis) $= 0.253$ nm with $\beta = 93°$.

2. Materials

For this study, two different VF_2/VF_3 copolymer compositions were used, 81/19 and 76/24 mol%. The 76/24 composition shows a clear splitting between the Curie and melting transitions while the 81/19 composition does not.

For the 76/24 mol% composition three films were analyzed. These films were retains taken from an extruded film which was then annealed between its Curie transition and melting and then poled. Thus the films are designated as after extrusion, after annealing and after poling.

For the 81/19 mol% composition both films and powders were analyzed. The films were made through a spin cast process from MEK and vacuum dried at 50°C. These films were then annealed and poled at different temperatures, times and AC electric fields. The temperature ranged from 134 to 140°C, the time was either 4 or 8 h while the poling field ranged from 4 to 6 kV/cm (for a ten-minute duration). A synopsis of the film processing is given in Table 2. Specimens of the powder were subjected to additional thermal treatments which include quenching from the melt and quenching from 136°C after being annealed for 15 h.

3. Experimental

The mol% of VF_3 in the VF_2/VF_3 copolymers was calculated from proton NMR spectra at 200 MHz. Molecular weight distributions were obtained on a Waters 150C ALC/GPC at 50°C with N-methyl pyrrolidone (stabilized with 0.05M LiBr) as the mobile phase. All molecular weights were determined relative to a polystyrene standard and no adjustment was made for polymer/solvent interactions. Apparent melt viscosities were determined by capillary rheology at a shear rate of 100 sec^{-1} at 232°C. Measurement of the piezoelectric strain coefficient d_{33} was made using a Berlincourt piezo d_{33} meter at 100 Hz. (In actuality since the sample is restricted at the point measured, the d_{33} reported should be considered an apparent d_{33}.)

For the 76/24 mol% process study a Perkin–Elmer DSC7 with an intracooler II attachment was used. For the 81/19 mol% studies a TA Instruments DSC 910 was used. Cooling was performed by either a mechanical cooling accessory (MCA) or cooling can. All measurements were made while the DSC cell was purged with nitrogen. Calibration was performed using high purity indium and lead. Sample masses of 9 to 10 mg were used.

For both the process and d_{33} studies a cycled DSC method was used. That is, all specimens were first cooled to −20°C then heated to 210°C where it was held for 10 min. The sample was cooled to −20°C and then reheated through the melt. A rate of 10°C/min was used for each ramp. Finally, for the cold crystallization study on the 81/19 mol% sample various heating rates from 2– 50°C/min were employed.

Lastly, a dynamic mechanical analysis (DMA) was performed on a 81/19 mol% specimen that had been molded into a bar and quenched from the melt. The specimen was heated 2°C/min and flexed at 1 Hz using a TA Instruments 983 unit. The DMA was calibrated using high purity metals that had been embedded in a plastic medium.

4. Results

4.1. Characterization and end use measurements

Table 1 provides the characterization data on the two resins. Table 2 lists the average d_{33} values

Table 1
Material's characterization

Mol% VF_3 from ^1H NMR	Mw GPC	Mw/Mn GPC	Melt viscosity at 100 sec^{-1} in Kilopoise
24	225.000	2.3	13.7
19			13.6–13.9

Table 2

Annealing temperature (°C)	Annealing time (h)	Poling field (kV/cm)	d_{33} pC/N (at 100 Hz)	Standard deviation
134	8	4	16.8	0.45
134	8	5	21.4	0.89
134	8	6	21.6	0.55
138	8	4	24.0	0
138	8	5	25.8	0.45
138	8	6	27.6	0.89
140	4	4	22.6	0.55
140	4	5	23.6	0.55
140	4	6	23.4	0.55
140	8	4	24.0	1.73
140	8	5	24.0	0
140	8	6	25.0	0.71

measured on the poled films. Five d_{33} measurements were made per processed film.

4.2. Thermal analysis

In Fig. 1 both Curie and melting transitions can be noted. Although the processing condition affects the transition region, the Curie transition occurs upon heating from approximately 75–125°C and the melting from approximately 125–150°C. Below the Curie transition is the LT phase and between the Curie and melting peaks is the HT phase.

The melting peaks are similar for the after annealing and after poling samples; however, the after extrusion sample shows a smaller peak height by approximately one-half, a slightly lower peak area, and a decrease in peak temperature by about 3 to 4°C as compared to the after annealing and after poling samples. The Curie transition of all three conditions is different. Annealing causes a decrease in the Curie peak temperature although poling increases it back with a much larger and sharper peak.

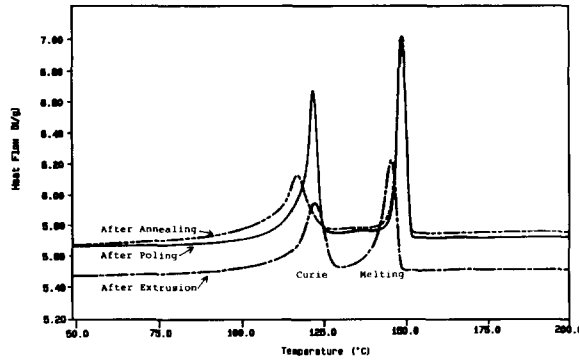

Fig. 1. DSC of the 76/24 mol % VF_2/VF_3 copolymers of retains taken after the extrusion, annealing and poling steps.

Analysis of the cooling and reheating traces indicates that all three film retains are similar compositionally. That is, the cooling and reheating are superimposable. Furthermore, the DSC fingerprints of the retains also match that of the pellets from which the retains were processed.

Scans at various rates were used to analyze a variety of thermal histories for the 81/19 composition. As seen in Figs. 2–5 an exotherm was observed in the powder and in the film but not in the annealed and quenched samples. The exotherm is dependent on the heating rate with the slower rates favoring its appearance. At the 50°C/min heating, the crystallization could not be differentiated even for the spin cast films. With the exception of the quenched samples, faster heating rates elevated the melting temperature while

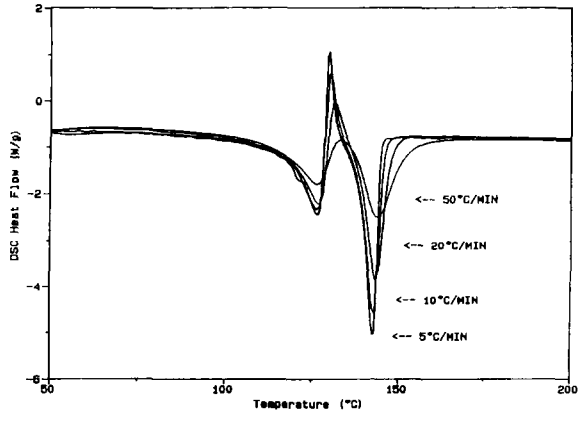

Fig. 2. Effect of heating rate on the DSC scans of spin cast film of a 81/19 mol% VF_2/VF_3 copolymer.

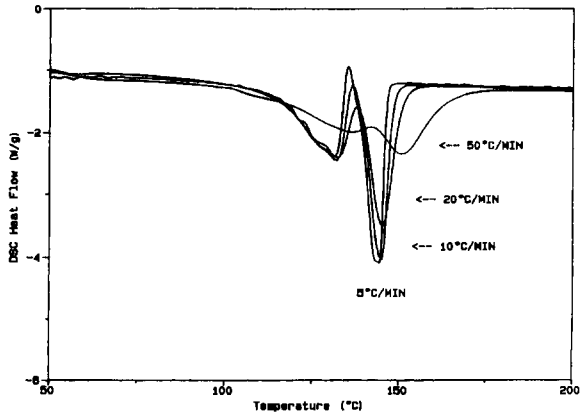

Fig. 3. Effect of heating rate on the DSC scans of powder of a 81/19 mol% VF_2/VF_3 copolymer.

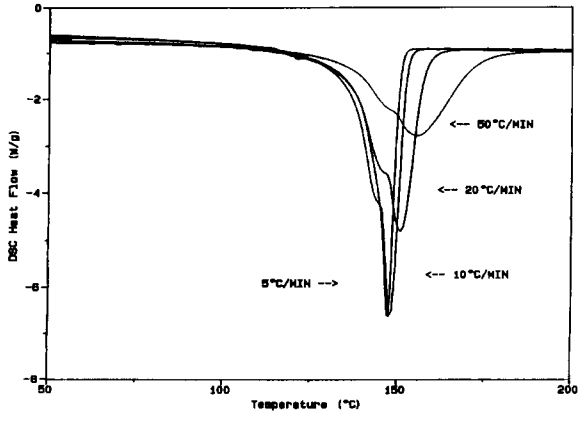

Fig. 4. Effect of the heating rate on the DSC scans of an annealed 81/19 mol% VF_2/VF_3 copolymer.

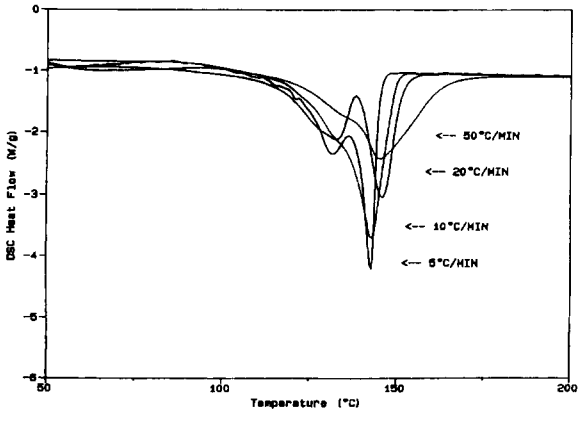

Fig. 5. Effect of heating rate on the DSC scans of powder that was quenched into liquid nitrogen from the melt.

Table 3
Glass transition temperatures with their associated Curie (T_c) and melting peak (T_m) temperatures

	T_g (°C)	ΔC_p (J/g °C)	T_c (°C)	T_m (°C)
Film	−29.7	0.074	126.9	143.9
Quenched powder	−34.0	0.080	135.3	145.1
Virgin powder	−28.9	0.070	136.4	150.5
Annealed powder	−21.9	0.036	147.8	155.7

slower rates allowed a better differentiation between the Curie and melting transitions.

Glass transition determinations were made for the 50°C/min heatings. For these runs the specimens were previously cooled rapidly through the glass transition using a nominal rate of 20°C/min from ambient temperature. The glass transitions were found to vary for the various thermal histories. Between the quenched and annealed samples a difference of 12°C was noted with the quenched specimen having the lowest T_g and the annealed specimen having the highest (see Table 3). The T_g seemed to be sensitive to changes in both the Curie and melting transitions and, in general, T_g increased with both the Curie and melting transitions. However, increases in the Curie transition with only slight changes in the melting temperature (film versus quenched powder) seemed to favor lowering the T_g while increases in the melting transition with only slight changes in the Curie transition (quenched powder versus virgin powder) seemed to favor raising the T_g. This seemingly incongruous behavior may be explained by two transitions overlapping each other. DMA of a quenched bar molded from the 81/19 mol % powder showed two overlapping relaxations with loss modulus peaks at −40 and 7°C (see Fig. 6). Hence, one might speculate that the transition seen by DSC encompasses two relaxations making the transition baseline unclear.

For the d_{33} study, d_{33} measurements were performed on the 81/19 mol % samples which had been processed to different piezoelectrical responses. The d_{33} measurements were correlated to various peak parameters. These parameters include peak height, peak height ratio (ratio of the heights of the melting peaks between the first and second heatings), heat of transition, and melting peak temperature. The correlations are presented in Figs. 7–10.

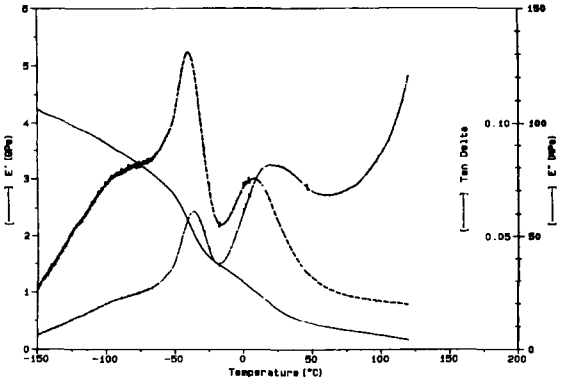

Fig. 6. DMA of an 81/19 mol% VF_2/VF_3 copolymer showing two prominent relaxations between −50 to 50°C.

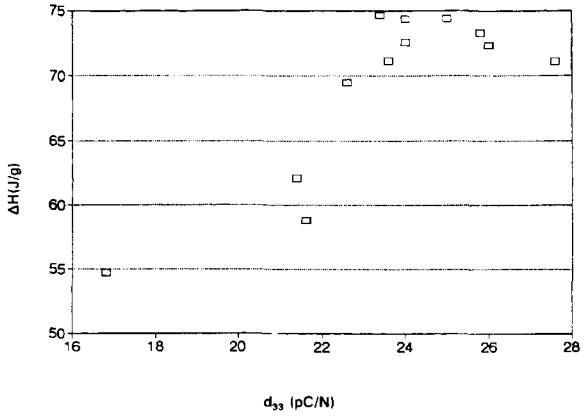

Fig. 9. Enthalpy versus d_{33} of poled spin cast films.

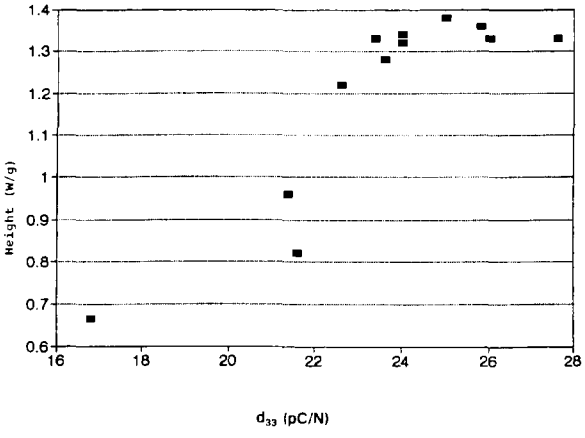

Fig. 7. Peak height versus d_{33} of poled spin cast films.

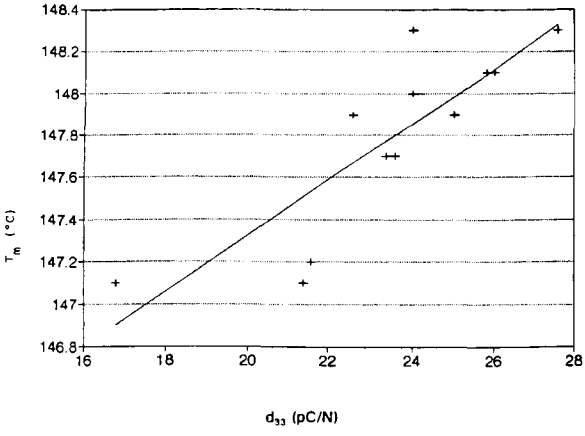

Fig. 10. Peak temperature versus d_{33} of poled spin cast films.

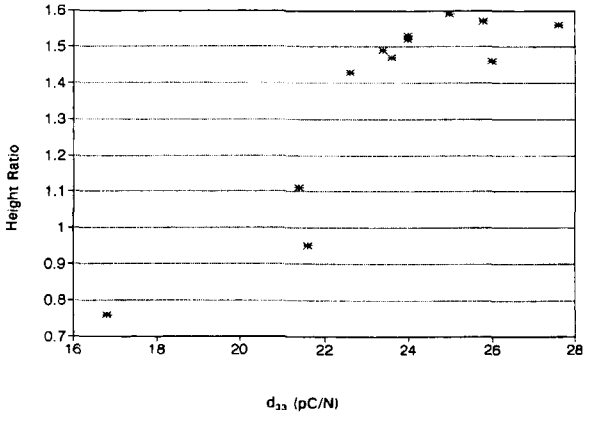

Fig. 8. Height ratio versus d_{33} of poled spin cast films.

5. Discussion

A possible interpretation of the DSC data for the 76/24 mol% runs is that upon extrusion poor crystallites are formed. The after extrusion sample's melting demonstrates all the symptoms of poorly defined crystals. This is evident from the lower melting temperature, shorter peak height, and broader peak base, as compared to the annealed and poled samples' melting peaks. The poor crystals are probably formed from quenching the resin from the melt during the extrusion process.

Annealing the extruded sample above the Curie transition but below the melting transition increased the amount of crystallinity and greatly increased the

size and perfection of the HT crystalline regions. This is evident from the higher melting peak temperature and peak height, and slightly larger peak area. However, since the Curie transition maintains approximately the same area but is now lower in temperature, annealing does not perfect the LT phase. Annealing instead seems to have the opposite effect on the LT phase even though the more 'less defect' HT phase is available from which the LT phase can be formed. However, the LT phase does not take advantage of this since the Curie peak shape and area remains almost unchanged. On the other hand, poling seems to be perfect and increase the LT phase thereby increasing the Curie peak in height and area, and narrowing the peak base.

As mentioned in the Introduction, the α phase is similar to the HT phase. Both the α phase and the HT phase have similar conformations as noted through spectroscopic studies [26]. However, the α phase can be poled and exhibits piezoactivity while the HT phase does not [4,30]. Based on dielectric and NMR data Tashiro et al. [16] concluded that the HT phase exhibits rotational motion along its chain axis. This additional mobility would thus explain the exotherm observed above the Curie transition where sufficient mobility exists for the molecules to reorganize or cold crystallize.

However, how can we explain this conformational disorder that would account for the paraelectricity of the HT phase? The condis crystal concept does this [31]. That is, the HT phase would best be described as a condis (conformationally disordered) crystal mesophase where a long range conformational disorder exists causing rotational randomization of the dipoles along the chain axis, thereby accounting for its paraelectricity. Thus the cold crystallization of the condis mesophase was previously prevented by an imperfect LT phase. (It should be noted that if the Curie transition is assigned as a condis or disordering transition, T_d, then the melting is best described as the temperature of isotropization, T_i [31].)

If one assumes that piezoactivity in VF_2/VF_3 copolymers is dependent on the orientation of dipoles in the crystalline phase then crystal perfection as well as crystallinity may be monitored through DSC. Correlations of both peak height and heats of transition to piezoactivity showed only a limited relationship. At 24 pC/N a plateau was quickly reached where increases in d_{33} did not have an associated increase in any DSC parameters (the peak temperature correlation evinced a large error and differentiation between a slight increase and a plateau effect was difficult to discern). This suggests that both the crystallinity and crystal perfection have a dominant effect on piezoactivity up to a certain point and then other factors become important.

6. Conclusions

Use of DSC to monitor the processing of VF_2/VF_3 copolymers in highly piezoelectric materials was investigated. DSC was found to follow the processing of the material. Although transition peak parameters were found to show a relationship with the piezoactivity for the 81/19 mol% a leveling effect was noted at high activities. Finally, a cold crystallization effect was noted for the 81/19 mol% copolymer which can be explained by the condis crystal concept.

Acknowledgements

Special thanks to James Mason for preparing and measuring the activities of the spin cast films. It also should be noted that parts of this paper were given at the 24th North American Thermal Analysis Society Conference.

References

[1] T. Yamada and T. Kutayama, J. Appl. Phys., 52 (1981) 6859.
[2] T. Furukawa, M. Date, E. Fukada, Y. Tajitsu and A. Chiba, Jpn. J. Appl. Phys., 19 (1980) L109.
[3] T. Kitayama, T. Ueda and T. Yamada, Ferroelectrics, 28 (1980) 301.
[4] A.J. Lovinger, in Developments in Crystalline Polymers, D.C. Bassett, Ed., Vol. 1, Applied Science, London, 1982, Chap. 5, 195.
[5] A.J. Lovinger, Macromolecules, 15 (1982) 40.
[6] B. Wunderlich, Macromolecular Physics, Vol. III, Crystal Melting, Academic Press, 1980.
[7] M. Bachmann, W.L. Gordon, S. Weinhold and J.B. Lando, J. Appl. Phys., 51 (1980) 5095.
[8] G.R. Davies and H. Singh, Polymer,, 20 (1979) 772.
[9] G.R. Davies, Inst. Phys. Conf. Ser. No., 58 (1981) 50.
[10] J.B. Lando, H.G. Olf, and A. Peterlin, J. Polym Sci.: Part A-1, 1966, 4, 941.

[11] R. Hasegawa, Y. Takahashi, Y. Chatani and H. Tadokoro, Polymer Journal, 1972, 3, No. 5, 600.
[12] A.J. Lovinger and R.E. Cais, Macromolecules, 1984 (1939) 17.
[13] Y. Higashihata, J. Sako and T. Yagi, Ferroelectrics, 32 (1981) 85.
[14] Ye. L. Gal'perin and Y.V. Strogalin, Polymer Science, USSR, 1965, 7, 15.
[15] R.R. Kolda and J.B. Lando, J. Macromol. Sci., -Phys., B11 (1975) 21.
[16] K. Tashiro, K. Takano, M. Kobayashi, Y. Chatani and H. Tadokoro, Ferroelectrics, 57 (1984) 297.
[17] Y. Oka and N. Koizumi, J. Polym. Sci.: Part B: Polym. Phys., 24 (1986) 2059.
[18] A.J. Lovinger, T. Furukawa, G.T. Davis and M.G. Broadhurst, Ferroelectrics, 50 (1983) 227.
[19] K. Tashiro and M. Kobayashi, Phase Transitions, 18 (1989) 213.
[20] K. Tashiro, K. Takano, M. Kobayashi, Y. Chatani and H. Tadokoro, Polymer, 25 (1984) 195.
[21] A.J. Lovinger, G.T. Davis, T. Furukawa and M.G. Broadhurst, Macromolecules, 15 (1982) 323.
[22] G.T. Davis, T. Furukawa, A.J. Lovinger and M.G. Broadhurst, Macromolecules, 15 (1982) 329.
[23] A.J. Lovinger, T. Furukawa, G.T. Davis and M.G. Broadhurst, Polymer, 24 (1983) 1225.
[24] A.J. Lovinger, T. Furukawa, G.T. Davis and M.G. Broadhurst, Polymer, 24 (1983) 1233.
[25] J.F. Legrand, Ferroelectrics, 91 (1989) 303.
[26] J.S. Green, J.P. Rabe and J.F. Rabolt, Macromolecules, 19 (1986) 1725.
[27] K. Tashiro, K. Takano, M. Kobayashsi, Y. Chatani and H. Tadokoro, Polymer, 22 (1981) 1312.
[28] A.J. Lovinger, D.D. Davis, R.E. Cais and J.M. Kometani, Polymer, 28 (1987) 617.
[29] T. Horiuchi, K. Matsushige and T. Takemura, Jpn. J. Appl. Phys., 25 (1986) L465.
[30] T. Yamada, T. Ueda and T. Kitayama, J. Appl. Phys., 52 (1981) 948.
[31] B. Wunderlich, 1990, Thermal Analysis, Academic Press, San Diego.